Biomechanics in the Inner Ear and Immune System

Hiroshi Wada

Professor
Department of Bioengineering and Robotics, Graduate School of Engineering
E-mail: wada@cc.mech.tohoku.ac.jp

Abstract

This report is divided into two parts, namely, biomechanics in the inner ear and that in the immune system. In the inner ear, the motor protein prestin densely embedded in the lateral membrane of outer hair cells (OHCs) play in important roles. To date, several researches aiming to clarify the structure of prestin have been conducted by electron microscopy (EM) and atomic force microscopy (AFM). However, such structure has remained unclear. In this study, an attempt was made to observe prestin in the plasma membrane of prestin-expressing cells using an experimental approach combining AFM with quantum dots (Qdots), used as topographic surface makers. As a result, ring-like structures, each with four peaks and one valley at its center, were recognized in the vicinity of Qdots, suggesting that there structures were prestin.

In the immune system, we analyzed the mechanism by which eosinophilic leukemia EoL-1 cells differentiate into mature eosinophils on exposure to *n*-butyrate. It has remained to be elucidated for about 20 years. The results showed that the activity of *n*-butyrate to inhibit histone deacetylase continuously induces the differentiation into mature eosinophils. This finding may contribute to the development of a novel treatment of eosinophilic leukemia.

1. Observation of the Motor Protein Prestin by AFM with Qdots

1.1. Introduction

Figure 1 shows a schematic of the human ear. Sound entering an eternal ear canal vibrates tympanic membrane. Such vibration is transmitted to cochlea via ossicles, resulting in the vibration of the organ of Corti. In the organ of Corti, there are two types of sensory hair cells, namely, inner hair cell (IHC) and OHC. The vibration of the organ of Corti changes the membrane potential of both hair cells. Due to such change, IHCs release the neurotransmitter. As a result, the signal is transmitted to the brain. Owing to this mechanism, we can finally hear the sound. On the other hand, the OHCs show their elongation and contraction in response to the change in membrane potential. This electromotility amplify the amplitude of the vibration of the organ of Corti, realizing the high sensitivity of mammalian hearing [1-4].

The OHC motility is considered to be driven by the conformational change of the motor protein prestin in the plasma membrane of OHCs [5]. Prestin-knockout and prestin mutant-knockin mice were created and then it was shown that these mutant mice showed significant hearing loss [6,7]. These results suggest that prestin play crucial role in high sensitivity of mammalian hearing. To date, for clarification of the structure of prestin, several researches have been carried out. EM and AFM of the plasma membrane of OHCs found that particles with diameter of 10 nm, probably indicating prestin, existed in such membrane [8-12]. On the other hand, in our laboratory, prestin stably-expressing Chinese hamster ovary (CHO) cells were created and then their plasma membranes were observed by AFM. As a result, ring-like structure with diameter of 8-12 nm possibly showing prestin could be found [13]. However, since there are many kinds of intrinsic membrane proteins other than prestin in the plasma membranes of OHCs and CHO cells, it was impossible to clarify which structures observed in such membranes were prestin. In this study, to overcome such a problem, an experimental approach combining AFM with Qdots, used as topographic surface markers, was employed. The plasma membranes of both types of CHO cells were subsequently observed by fluorescence microscopy and then scanned by AFM.

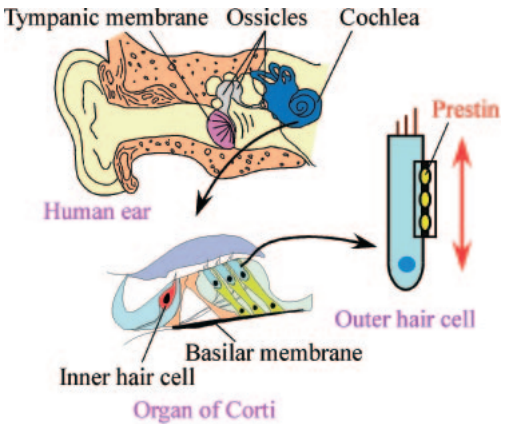

Fig. 1. Human auditory system. Sensory cells, such as outer hair cells (OHCs), inner hair cells and various kinds of the other cells, sit on the basilar membrane. OHCs subject the membrane to force, leading to cochlear amplification, resulting in the high sensitivity of mammalian hearing. Prestin is thought to be the origin of the motility of OHCs.

1.2. Materials and methods

1.2.1. Cell culture

Prestin-transfected and untransfected CHO cells were used. The prestin-transfected CHO cells were constructed by transfection of gerbil prestin cDNA into CHO cells using pIRES-hrGFP-1a mammalian expression vectors (Stratagene, La Jolla, CA). Those expression vectors contain humanized *Renilla reniformis* green fluorescent protein (hrGFP) gene, which is connected to the prestin gene. CHO cell lines which stably express prestin were established using transfected cells by limiting dilution cloning [14,15]. The prestin-transfected and untransfected CHO cells were cultured in RPMI-1640 medium with 10% fetal bovine serum, 100 U penicillin/ml and 100 μg streptomycin/ml at 37°C with 5% CO_2.

1.2.2. Isolation of plasma membrane

The inside-out plasma membranes, i.e., cytoplasmic face is up, were isolated from the prestin-transfected CHO cells. The culture medium was removed and the cells were detached from a flask by incubation with 100 μM ethylenediamine tetraacetic acid (EDTA) in PBS (EDTA-PBS) solution for 5 min at 37°C. The EDTA-PBS solution containing the cells was put into a tube and centrifuged at 250 × *g* for 5 min. The supernatant was then removed and the culture medium was put into the tube. The culture medium containing the cells was agitated by pipetting in that tube and deposited on glass-bottomed dishes (Asahi Techno Glass, Chiba, Japan). After overnight culture, most of the cells had become reattached and spindle-shaped on the substrate. The culture medium was discarded and the cells were washed twice with an external solution (145 mM NaCl, 5.8 mM KCl, 1.3 mM $CaCl_2$, 0.9 mM $MgCl_2$, 10 mM HEPES, 0.7 mM Na_2HPO_4 and 5.6 mM glucose; pH 7.3) warmed to 37°C for removal of unwanted materials, such as cell fragments and proteins contained in the culture medium attached to the surfaces of the cells and substrate. The dish was immersed for 3 min in a hypotonic buffer (10 mM PIPES, 10 mM $MgCl_2$, 0.5 mM EGTA; pH 7.2), which had been cooled to 4°C. The cells were then sheared open by gentle exposure to a stream of the hypotonic buffer using a 1-ml pipette (Gilson, Villiers, France) several times, resulting in the isolation of the inside-out basal plasma membranes. After the isolated plasma membranes had been washed with PBS three times, they were incubated with a high-salt buffer (2 M NaCl, 2.7 mM KCl, 1.5 mM KH_2PO_4, 1 mM Na_2HPO_4; pH 7.2) for 30 min at room temperature to remove the cytoskeletal materials and the peripheral proteins [25]. The isolated membranes were then incubated with 0.05% trypsin for 1 min at room temperature to remove the remaining materials. Whether the plasma membrane could be isolated was confirmed by DiI staining.

1.2.3. Prestin labeling with Qdots

The isolated plasma membranes were fixed with 4% paraformaldehyde in PBS for 30 min at room temperature. After fixation, the membranes were rinsed three times with PBS and incubated with Block Ace (Dainippon Pharmaceutical, Osaka, Japan) for 30 min at 37°C. After PBS washing, the membranes were incubated with goat anti-prestin N-terminus primary antibody (Santa Cruz Biotechnology, Santa Cruz, CA) at a dilution of 1:100 in PBS overnight at 4°C. The membranes were then washed with PBS and incubated with Qdot®655-conjugated rabbit anti-goat IgG secondary antibody (Invitrogen, Carlsbad, CA) at a dilution of 1:200 in PBS for 60 min at 37°C. Finally, the membranes were washed with Hanks' balanced salt solution (HBSS; 5.33 mM KCl, 0.44 mM KH_2PO_4, 137.93 mM NaCl, 0.34 mM Na_2HPO_4, 0.56 mM glucose; pH 7.3) and immersed in this solution filtered with a 0.22-μm pore-size syringe filter (Millipore, Billerica, MA).

1.2.4. Atomic force microscopy

An AFM (NVB100, Olympus), in which the AFM unit is mounted on an inverted fluorescence microscope (IX70, Olympus), was used. A V-shaped silicon nitride cantilever (OMCL-TR400PSA-2, Olympus) with a spring constant of 0.02 N/m was used. To minimize sample damage during scanning, AFM images were obtained using the oscillation imaging mode (Tapping mode™, Digital Instruments, Santa Barbara, CA). By scanning the sample with this mode, height images of the sample surface were obtained. For all AFM images, the samples were scanned from left to right. Each scan line had 512 points of data, and an image consisted of 512 scan lines.

In the present study, Qdots were used as topographic surface markers. As the prestin molecules were labeled with primary and secondary antibodies, the distance between a Qdot and a prestin molecule was estimated to be ~20 nm [16]. The primary antibody used in this study reacts with the cytoplasmic N-terminus of prestin. Since such terminus consists of ~100 a.a., its length was estimated to be ~31 nm [17]. Assuming the antibody binds to the tip of the N-terminus, the estimated maximum distance between a Qdot and a prestin molecule is ~50 nm. Therefore, all structures observed within 66.5 nm apart from the center of a Qdot (i.e., 133 nm-square scanning area) were subjected to subsequent size analysis.

1.3. Results

1.3.1. Plasma membrane isolation and Qdots staining

Figure 3 shows a fluorescence image of isolated plasma membrane stained by DiI. Parts producing red

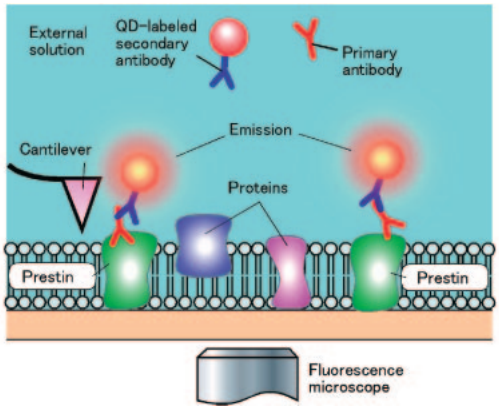

Fig. 2. Immune AFM of the isolated inside-out plasma membrane of the prestin-transfected CHO cell.

fluorescence are the plasma membrane. It could be confirmed that the cells were ruptured and then the plasma membranes were isolated.

Figure 4 shows the prestin labeling with Qdots of the isolated plasma membranes of a prestin-transfected CHO cell and those of an untransfected CHO cell. Prestin labeling (red), which labels the N-terminus of prestin, was observed in the isolated plasma membrane of the prestin-transfected CHO cell, by contrast, it was not observed in the isolated plasma membrane of the untransfected CHO cell. These results indicate the presence of prestin in the isolated plasma membranes of the prestin-transfected CHO cell even after the isolated plasma membranes were sonicated and incubated with the high salt buffer and trypsin.

1.3.2. Effects of scanning by AFM on Qdots

When the sample is scanned by AFM, the cantilever contacts Qdots. Hence, it was possible that the position of Qdots was changed during the scanning. Whether

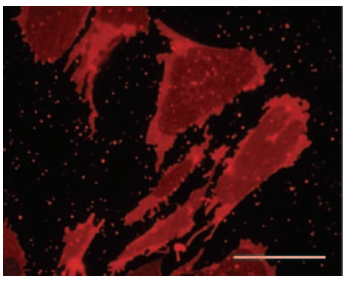

Fig. 3. Fluorescence image of isolated plasma membrane of CHO cells. The isolated plasma membranes were stain by CM-DiI, which is a fluorescence lipophilic membrane probe. It can be confirmed that the cells were sheared open, thus becoming an isolated plasma membrane. Scale bar shows 20 μm.

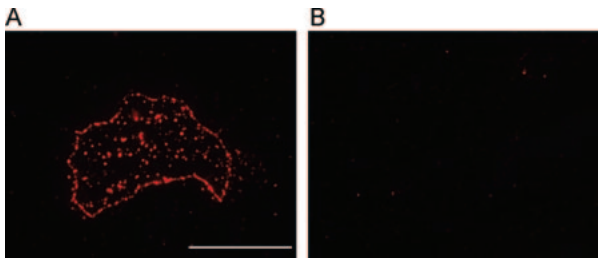

Fig. 4. Qdot labeling of isolated plasma membrane of CHO cells. A. Isolated plasma membrane of prestin-transfected CHO cell. B. Isolated plasma membrane of prestin-untransfected CHO cell. Fluorescence of Qdot was observed in the prestin-transfected CHO cell, but not observed in the untransfected CHO cell. Scale bar represents 20 μm.

the position of Qdot was changed or not before and after the scanning was investigated. Figure 5 shows a fluorescence image of Qdots labeled plasma membrane before and after the scanning and low-magnification AFM image. As the fluorescence image unchanged, effects of the cantilever on the position of Qdots were considered to be ignorable.

1.3.3. Observation of prestin by AFM

Figure 6 shows the high-magnification 3-D AFM images of the boxed area shown in the low-magnification AFM image of Fig. 5. Qdots 8 nm in height were clearly observed on the cytoplasmic face of the isolated plasma membrane of the prestin-transfected CHO cell, as indicated by black arrowheads. As shown in the magnification at the right of Fig. 6, a ring-like structure with four peaks and one valley at its center, possibly corresponding to a prestin molecule, was observed in the vicinity of the Qdot (a, arrow). In the vicinity of the other Qdots, similar structures were observed at the location indicated by arrows (a-d), the magnifications of which are shown in the bottom panels.

1.4. Discussion

1.4.1. Sample preparation

In our previous study, the cytoplasmic surfaces of the isolated plasma membranes of CHO cells were found to be covered with protruding globular structures ~100 nm in diameter [13]. These protruding globular structures were colocalized with the immunofluorescence of prestin, indicating that prestin was not uniformly distributed in the plasma membrane of the prestin-transfected CHO cells. As these large structures hinder efforts to obtain AFM images at high-magnification, the images were obtained in the membrane areas without such structures in that study. In the present study, to observe the membrane topology

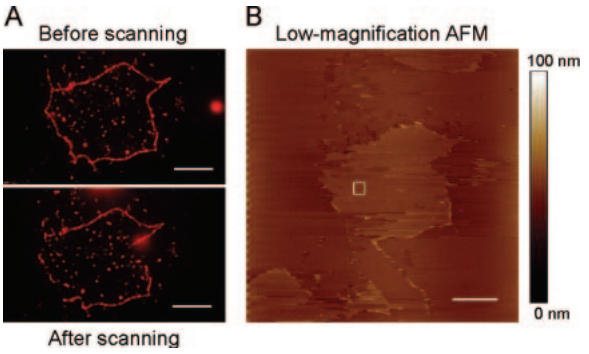

Fig. 5. Isolated Inside-out plasma membrane of the prestin-transfected CHO cell. A. Fluorescence image of Qdots labeling prestin. Fluorescence of Qdots was observed before and after scanning with the AFM, indicating that the existence of Qdots on the scanned area. B. Low magnification AFM image. Scale bars are 10 μm.

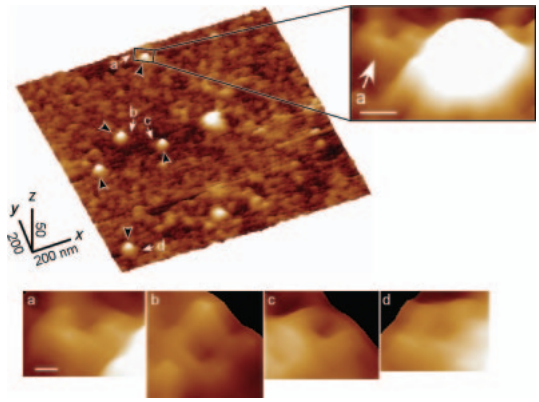

Fig. 6. High-magnification 3-D AFM images of prestin on the plasma membrane of the prestin-transfected CHO cells. Qdots were indicated by black arrowheads. A squarish ring-like structure with four peaks and one valley at its center, possibly corresponding to a prestin molecule, was observed in the vicinity of the Qdot (white arrow). Similar structures were observed at the location indicated by arrows (a-d). Scale bars at the right and bottom are 20 and 10 nm, respectively. Reprinted from [18] with the kind permission of Springer Science+Business Media.

of prestin at the nano-scale level, a flatter surface of the isolated plasma membrane was required. To obtain such flat plasma membrane sheets, therefore, the sample preparation method was modified. That is, the CHO cells were cultured in the culture medium overnight, rather than 5-min incubation in the external solution just before the sonication as in the previous method. Due to this, the cell shape became flatter and more spindly, compared with the cells grown by the previous method. As shown in Fig. 5B, this procedure significantly reduced the number of the protruding globular structures 100 nm in diameter on the cytoplasmic faces of the isolated plasma membranes of the CHO cell. CHO cells attached to the extracellular matrix are flattened into a spindle shape by using a membrane glycoprotein fibronectin receptor, a member of the integrin superfamily. This membrane protein forms focal adhesions that link the extracellular matrix to actin microfilaments and a number of cytoskeleton proteins. Flattening is then achieved by dynamic formation of adhesion sites at the cell periphery in equilibrium with free fibronectin receptors subjected to the endocytic cycle and internalized into the cytoplasm. After overnight culture of CHO cells, in the present study, the cells have become spindle-shaped and the formation of the vesicles required for assembly and/or disassembly of the focal adhesions had possibly ceased. Consequently, the number of vesicles was reduced, thus leading to a significant reduction of the protruding globular structures on the cytoplasmic sides of the isolated plasma membranes of the CHO cells.

The existence of prestin in the plasma membrane isolated from such spindle-shaped CHO cells after incubation with high-salt buffer and trypsin was confirmed by immunostaining (Fig. 4). Fluorescence labeling of the prestin-transfected CHO cells but not of the untransfected CHO cells was confirmed, suggesting that prestin existed in the isolated plasma membranes of the spindle-shaped CHO cells even after treatment with high-salt buffer and trypsin, and thus these isolated plasma membranes were applicable as samples for AFM observation.

1.4.2. The structure of prestin

In the present study, Qdots were used as topographic surface markers. Assuming the primary antibody binds at the tip of the N-terminus and the secondary antibody conjugated with Qdot connects to the primary antibody, the maximum distance between a Qdot and a prestin molecule is estimated to be ~50 nm. As shown in Fig. 6, Qdots 8 nm in height were clearly observed on the cytoplasmic face of the isolated plasma membrane of the prestin-transfected CHO cell (black arrowheads). The magnification shown on the right revealed that a ring-like structure about 10 nm in diameter with four peaks and one valley at its center, possibly corresponding to a prestin molecule, existed in the vicinity of the Qdot. Such structures were also observed in the vicinity of Qdots indicated by arrow (a-d, Fig. 6). Similarly-shaped structures were also observed in the vicinity of Qdots on the cytoplasmic faces of the plasma membranes isolated from other prestin-transfected CHO cells.

This study attempted to clarify the structure of presitn by AFM, while Mio et al. tried to do by EM [19]. According to their report, prestin is a bullet-shaped particle with a small protrusion at its center which extends into the cytoplasm. In the present study, we isolated the inside-out plasma membranes of the prestin-transfected CHO cells and then imaged the cytoplasmic faces of such membranes. On this side, we observed ring-like structures, each with a

depression at its center and four surrounding peaks, as shown in Fig. 6. The difference may be due to the difference in observation techniques, the main difference being the force applied to prestin molecules. In the present study, the sample was scanned by the cantilever, the spring constant of which was 0.02 N/m. During the scanning, as the distance between the tip of the cantilever and the sample was controlled so as to reduce the amplitude of the cantilever oscillation by ~2-5 nm during scanning, the force applied to the sample could be roughly estimated to be ~40–100 pN based on Hooke's law if the load applied to the sample is assumed to be static. In reality, however, since the cantilever was oscillated during scanning, this load was more like dynamic, suggesting that the force applied to the sample was at least twice larger than such estimation. On the other hand, transmission electron microscopy does not load such force on the sample. According to the report by Mio et al., protein density seemed to be high in the outermost region of the prestin molecule and low inside. They therefore proposed the possibility of the existence of a protein-sparse cavity inside the prestin molecule. Such a configuration of the prestin molecule implies the flexibility of its small cytoplasmic protrusion. Recently, single molecule force spectroscopic studies using AFM have demonstrated that a higher-order structure of protein is unfolded when a monomeric unit of protein is stretched at a force of ~100 pN [20]. Assuming the flexibility of the cytoplasmic protrusion of prestin and considering the ~40–100-pN or more force applied to the sample by the AFM cantilever, the possibility of deformation of this protrusion into its interior during AFM imaging cannot be ruled out. Due to this, the cytoplasmic part of prestin was presumably imaged to be the ring-like structures, each with a depression at its center surrounded by four peaks instead of with a small protrusion at its center.

1.5. Conclusions

Prestin molecules expressed in the plasma membranes of prestin-transfected CHO cells were labeled with Qdots, and those dots about 8 nm in height were clearly imaged by AFM. Ring-like structures, each with four peaks and one valley at its center, were observed in the vicinity of the Qdots, suggesting that prestin forms a tetramer in the plasma membranes of the prestin-transfected CHO cells.

2. Differentiation of Eosinophilic Leukemia EoL-1 Cells into Eosinophils Induced by Histone Deacetylase Inhibitors

2.1. Introduction

Chromatin comprises repeating units of nucleosome core particles and linker DNA [21]. The particles consist of an octamer of core histone containing two molecules of each histone, H2A, H2B, H3 and H4, around which 145 bp of DNA are wrapped in 1.75 turns [22,23]. In gene expression, histones in the nucleosome core particles are acetylated at the ε-amino group of specific lysine residues of the N-terminus by histone acetyltransferases (HAT) [23]. The acetylated lysine residues are deacetylated by histone deacetylases (HDAC) [24]. Therefore, the acetylation by HAT and the deacetylation by HDAC play important roles in cellular function by controlling the level of gene expression.

Recently, natural and synthetic compounds with the ability to inhibit HDAC activity have been reported [25, 26]. These HDAC inhibitors used in this experiment is the short-chain fatty acids *n*-butyrate [27], the hydroxamic acid trichostatin A (TSA) [28], the cyclic tetrapeptide apicidin [29] (Fig. 7). The acetylation by HAT is sustained while HDAC are inhibited by HDAC inhibitors, resulting in an accumulation of acetylated histones that induces various biological activities including differentiation, proliferation, and apoptosis via gene expression [25].

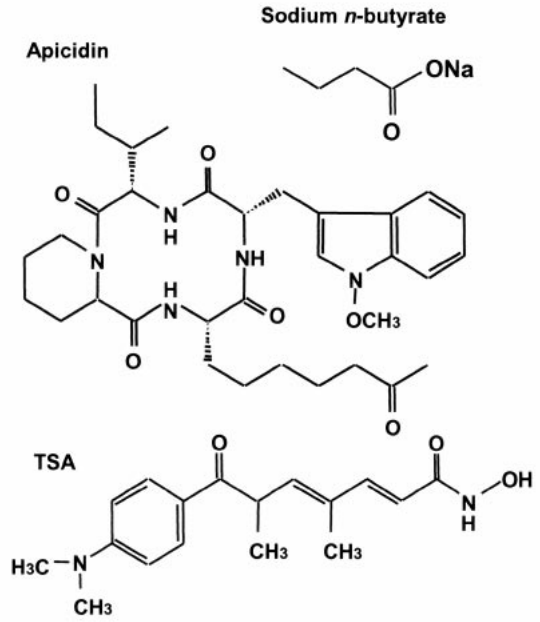

Fig. 7. Chemical structures of sodium *n*-butyrate, apicidin and TSA.

The development and function of eosinophils under conditions of allergic inflammation such as bronchial asthma have also been studied using eosinophilic leukemia cell lines such as HL-60 clone 15 cells and EoL-1 cells [30-32]. It has been reported that *n*-butyrate induces the differentiation of EoL-1 cells [33]. However, the mechanism by which these cells differentiate into mature eosinophils on exposure to *n*-butyrate has remained to be elucidated for about 20 years. Therefore, in this study, we analyzed the mechanism behind the differentiation of EoL-1 cells into mature eosinophils using the HDAC inhibitors apicidin, TSA and *n*-butyrate.

2.2. Materials and methods

2.2.1. Cell culture

Eosinophilic leukemia EoL-1 cells (5 x 10^4 /ml) were incubated at 37˚C for different time points as indicated in RPMI-1640 medium (pH 7.8) containing various concentrations of apicidin, TSA or *n*-butyrate .

2.2.2. Proliferation assay

EoL-1 cells were incubated at 37˚C for different time points as indicated in medium containing various concentrations of each drug. After the incubation, the viable cells were enumerated using a hemocytometer.

2.2.3. Western blotting

The cell lysate was subjected to electrophoresis on a 15% acrylamide gel for 2 h at 125 V and the proteins separated in the gels were transferred onto a nitrocellulose membrane and blocked in a blocking solution for 1 h at room temperature. The membrane was incubated for 12 h at 4˚C with 1st antibody. After 4 washes with T-TBS, the membrane was incubated at 4˚C for 3 h with biotinylated 2nd antibody. The reaction products were incubated for 30 min at room temperature with Vectastain ABC reagent and visualized using the Chemiluminescence Detection System. The membrane was exposed to Kodak X-Omat AR film.

2.2.4. Flowcytometry

For the analysis of viability, the cells were incubated for 30 min at room temperature in 0.1 ml of PBS containing 2 µg of 7-amino-actinomycin D (7-AAD, Sigma). For the detection of CCR3, the cells were incubated with phycoerythrin (PE)-labeled anti-human CCR3 for 30 min at 4˚C. The fluorescence of the cells (1 x 10^4) was analyzed with a flowcytometer.

2.2.5. Statistical analysis

The statistical significance of the results was analyzed using Dunnett's test for multiple comparisons.

2.3. Results

2.3.1 Effects of HDAC inhibitors on the proliferation of EoL-1 cells

To clarify whether apicidin, TSA, and *n*-butyrate inhibit the proliferation of EoL-1 cells, the number of cells after the incubation with these HDAC inhibitors was counted. As shown in Fig. 8, EoL-1 cells proliferated in a time-dependent manner during 8 days of incubation in the absence of HDAC inhibitors. Apicidin at 100 nM and *n*-butyrate at 500 µM significantly inhibited the proliferation of EoL-1 cells until day 8. On treatment with TSA at 30 nM, significant inhibition of the proliferation of EoL-1 cells was observed on days 2 and 4 but not on days 6 and 8 (Fig. 8).

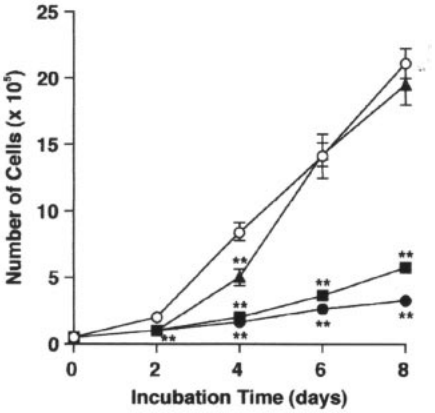

Fig. 8. Effects of apicidin, TSA, and *n*-butyrate on the growth of EoL-1 cells. EoL-1 cells were incubated for the periods indicated at 37˚C in the absence (open circles) or presence of 100 nM apicidin (closed circles), 30 nM TSA (closed triangles), or 500 µM *n*-butyrate (closed squares). Values are the means from three samples with the S.E.M. Statistical significance: $^{**}p < 0.01$ vs. the corresponding control.

2.3.2. Effects of HDAC inhibitors on the viability of EoL-1 cells

On treatment with apicidin at 10-100 nM, TSA at 10 and 30 nM, or *n*-butyrate at 500 µM, no significant change in the viability of EoL-1 cells was observed (Fig. 9). At higher concentrations of apicidin (300 and 1000 nM) and TSA (100 nM), the viability was significantly decreased (Fig. 9).

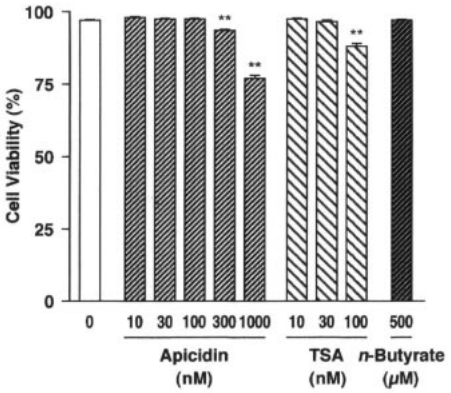

Fig. 9. Effects of apicidin, TSA, and *n*-butyrate on the viability of EoL-1 cells. EoL-1 cells were incubated for 1 day at 37˚C in medium containing the indicated concentration of apicidin, TSA, or *n*-butyrate. The viability of the cells was determined by flowcytometry using 7-AAD. Values are the means from three samples with the S.E.M. Statistical significance: $^{**}p < 0.01$ vs. the control.

2.3.3. Effects of HDAC inhibitors on the acetylation of histone H4 in EoL-1 cells

To clarify whether apicidin, TSA, and *n*-butyrate inhibit HDAC in EoL-1 cells, we determined the levels of acetylated-histone H4 by Western blotting. As shown in Fig. 9, treatment of EoL-1 cells with 100 nM of apicidin or 500 μM of *n*-butyrate dramatically induced the acetylation of histone H4. However, the acetylation of histone H4 by TSA at 30 nM reached a peak at 4 h and then declined until 48 h (Fig. 9A and B).

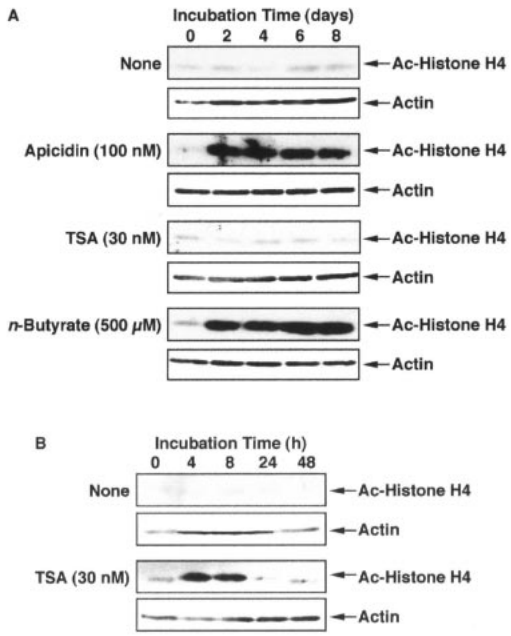

Fig. 10. Effects of apicidin, TSA, and *n*-butyrate on the acetylation of the histone H4. EoL-1 cells were incubated for the periods indicated at 37˚C in the presence or absence of apicidin (100 nM), TSA (30 nM), or *n*-butyrate (500 μM). The experiment shown is a representative of 3 independent experiments.

2.3.4. Effects of HDAC inhibitors on the expression of $p27^{kip1}$ in EoL-1 cells

We next examined the effects of apicidin, TSA, and *n*-butyrate on the expression of the cyclin-dependent kinase inhibitor $p27^{Kip1}$ by Western blotting. Apicidin at 100 nM and *n*-butyrate at 500 μM continuously induced the expression of $p27^{Kip1}$ until day 8 (Fig. 11). In contrast, the expression of $p27^{Kip1}$ induced by TSA at 30 nM reached a maximum at 24 h and decreased at 48 h (Fig. 11).

2.3.5. Effects of HDAC inhibitors on the expression of CCR3 on EoL-1 cells

After 8 days of incubation, apicidin at 100 nM and *n*-butyrate at 500 μM induced the expression of the markers of eosinophils CCR3 on EoL-1 cells (Fig. 12).

2.4. Discussion

EoL-1 cells, which were established from a patient with eosinophilic leukemia in 1985, have been utilized for studies on eosinophilic leukemia [33]. The development and function of eosinophils under conditions of allergic inflammation such as bronchial asthma have also been studied using EoL-1 cells [30, 31], because the cells differentiate into mature eosinophils when exposed to *n*-butyrate [33].

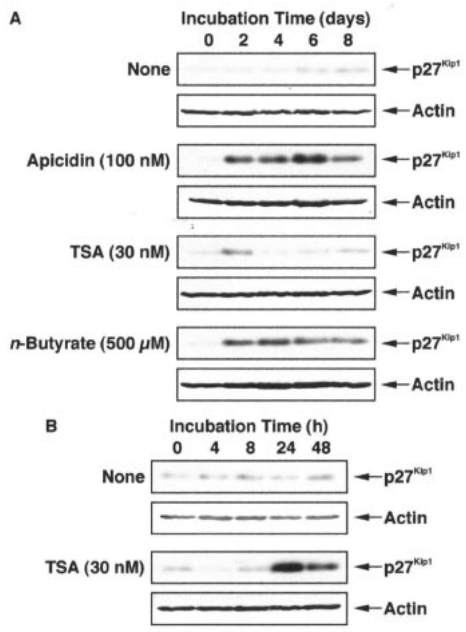

Fig. 11. Effects of apicidin, TSA, and *n*-butyrate on the expression of $p27^{Kip1}$ in EoL-1 cells. EoL-1 cells were incubated at 37˚C for the periods indicated in the presence or absence of apicidin (100 nM), TSA (30 nM), or *n*-butyrate (500 μM). The experiment shown is a representative of 3 independent experiments.

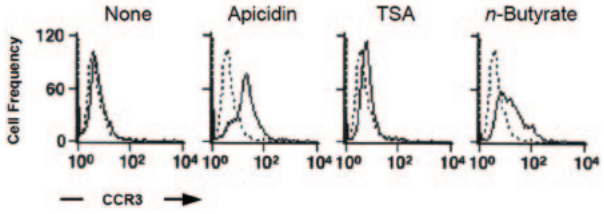

Fig. 12. Effects of apicidin, TSA, and *n*-butyrate on the differentiation of EoL-1 cells into eosinophils. EoL-1 cells were incubated for 8 days at 37˚C in medium containing the indicated concentration of apicidin, TSA, or *n*-butyrate. The expression of CCR3 was determined by flowcytometry. Dotted and solid lines represent the histogram before and after incubation with the drug, respectively. The experiment shown is a representative of 3 independent experiments.

Clarification of the mechanism behind this differentiation may contribute to the development of a novel treatment for eosinophilic leukemia and for inhibition of the differentiation of stem cells into mature eosinophils in individuals with allergic diseases.

It is reported that the half-life of TSA in cell cultures is 14.7 h [34], and the differentiation of HL-60 clone 15 cells into eosinophils was induced by repeated treatment (more than 3 times at an interval for 12 h) with TSA at 30 nM [32], suggesting that TSA has no activity to induce EoL-1 cells to differentiate into eosinophils due to its short half-life. In this study, we found that (1) *n*-butyrate and apicidin induces the continuous acetylation of histone H4 and has activity to induce the differentiation of EoL-1 cells into eosinophils, (2) apicidin at 100 nM is as effective as *n*-butyrate at 500 μM, and (3) TSA has no influence on the differentiation of EoL-1 cells into eosinophils due to its transient effect on the acetylation of histone H4. Therefore, we suggest that the continuous acetylation of histone H4 induces the differentiation of EoL-1 cells into eosinophils. These findings indicate that the continuous inhibition of HDAC activity induces the differentiation of EoL-1 cells into eosinophils, and suggest that the induction of EoL-1 cells into eosinophils on exposure to *n*-butyrate is due to the continuous inhibition of HDAC activity by *n*-butyrate.

Enhanced acetylation of histones and transcription factors in EoL-1 cells exposed to apicidin or *n*-butyrate leaded to the differentiation of these cells into eosinophils. It is thought that HDAC inhibitors have an ability to induce the differentiation of precursor cells into mature cells, and the maturation could be promoted by changes in the endogenous balance of HATs and HDACs in leukemia cells [26]. Furthermore, the mechanism behind the cell differentiation induced by HDAC inhibitors might be specific to the type of cell, because as we reported, in HL-60 cells, apicidin and TSA induced the early stage differentiation into CD11b-expressing cells and not the complete maturation to neutrophils or monocytes [35]. In erythroleukemia K562 cells, apicidin and *n*-butyrate induce differentiation into fetal hemoglobin-producing cells but not into CD11b-expressing cells [35-37], and the differentiation of K562 cells stimulated by apicidin is irreversible [37] whereas the differentiation of HL-60 clone 15 cells was reversible [32]. These findings suggest that the mechanism behind the cell differentiation is regulated by not only the acetylation of histone but also the endogenous cell-specific ability to differentiate into each lineage. As described above, our studies also suggest a difference in the ability of differentiation of the EoL-1 cells and HL-60 clone 15 cells [32] by using HDAC inhibitors. Therefore, we also suggest that HDAC inhibitors are applicable to the diagnosis of leukemia, for example, in the detailed identification of the type of leukemia cell. Therefore, clarification of the mechanism regulating the balance between HAT and HDAC activities would contribute to the development of a novel treatment of eosinophilic leukemia and allergic inflammation.

2.5. Conclusion

In conclusion, we have demonstrated that apicidin and *n*-butyrate inhibit proliferation and induce the differentiation of EoL-1 cells into eosinophils. These effects may be related to continuous acetylation of histone H4 induced by apicidin and *n*-butyrate as shown here. HDAC inhibitor therapy would have an effect on people suffering from eosinophilic leukemia since proliferation is inhibited and differentiation is induced, but it has not been tested thus far

Acknowledgements

Hiroshi Wada acknowledges the support of Tohoku University Global COE Program "Global Nano-Biomedical Engineering Education and Research Network Centre," as well as that of the following grants: Gtrant-in-Aid for Scientific Research on Priority Areas 15086202 from the Ministry of Education, Culture, Sports, Science and Technology of Japan, Grant-in-Aid for Scientific Research (B) 18390455 from the Japan Society for the Promotion of Science, that of Grant-in-Aid for Exploratory Research 18659495 from the Ministry of Education, Culture, Sports, Science and Technology of Japan, the Human Frontier Science Program, a Health and Labour Science Research Grant from the Ministry of Health, Labour and Welfare of Japan, the Iketani Science and Technology Foundation and the Daiwa Securities Health Foundation.

References

[1] Brownell WE, Bader CR, Bertrand D, and de Ribaupierre Y. Evoked mechanical responses of isolated cochlear outer hair cells. *Science* **227**, 194-196, 1985.

[2] Kachar B, Brownell WE, Altschuler R, and Fex J. Electrokinetic shape changes of cochlear outer hair cells. *Nature* **322**, 365-368, 1986.

[3] Ashmore JF. A fast motile response in guinea-pig outer hair cells: the cellular basis of the cochlear amplifier. *J Physiol* **388**, 323-347, 1987.

[4] Santos-Sacchi J and Dilger JP. Whole cell currents and mechanical responses of isolated outer hair cells. *Hear Res* **35**, 143-150, 1988.

[5] Zheng J, Shen W, He DZ, Long KB, Madison LD, and Dallos P. Prestin is the motor protein of cochlear outer hair cells. *Nature* **405**, 149-155, 2000.

[6] Liberman MC, Gao J, He DZZ, Wu X, Jia S, and Zuo j. Prestin is required for electromotility of the outer hair cell and the cochlear amplifier. *Nature* **419**, 300-304 2002.

[7] Dallos P, Wu X, Cheatham MA, Gao J, Zheng J, Anderson CT, Jia S, Wang X, Cheng WH, Sengupta S, He DZZ, and Zuo J. Prestin-based outer hair cell motility is necessary for mammalian cochlear amplification. *Neuron* **58**, 333-339, 2008.

[8] Arima T, Kuraoka A, Toriya R, Shibata Y, and Uemura T. Quick-freeze, deep-etch visualization of the 'cytoskeletal spring' of cochlear outer hair cells. *Cell Tissue Res* **263**, 91-97, 1991.

[9] Forge A. Structural features of the lateral walls in mammalian cochlear outer hair cells. *Cell Tissue Res* **265**, 473-483, 1991.
[10] Kalinec F, Holley MC, Iwasa KH, Lim DJ, and Kachar B. A membrane-based force generation mechanism in auditory sensory cells. *Proc Natl Acad Sci U S A* **89**, 8671-8675, 1992.
[11] Souter M, Nevill G, and Forge A. Postnatal development of membrane specialisations of gerbil outer hair cells. *Hear Res* **91**, 43-62, 1995.
[12] Le Grimellec C, Giocondi MC, Lenoir M, Vater M, Sposito G, and Pujol R. High-resolution three-dimensional imaging of the lateral plasma membrane of cochlear outer hair cells by atomic force microscopy. *J Comp Neurol* **451**, 62-69, 2002.
[13] Murakoshi M, Gomi T, Iida K, Kumano S, Tsumoto K, Kumagai I, Ikeda K, Kobayashi T, and Wada H. Imaging by atomic force microscopy of the plasma membrane of prestin-transfected Chinese hamster ovary cells. *J Assoc Res Otolaryngol* **7**, 267-278, 2006.
[14] Iida K, Konno K, Oshima T, Tsumoto K, Ikeda K, Kumagai I, Kobayashi T, and Wada H. Stable expression of the motor protein prestin in Chinese hamster ovary cells. *JSME Int J* **46C**, 1266-1274, 2003.
[15] Iida K, Tsumoto K, Ikeda K, Kumagai I, Kobayashi T, and Wada H. Construction of an expression system for the motor protein prestin in Chinese hamster ovary cells. *Hear Res* **205**, 262-270, 2005.
[16] Hartmann WK, Saptharishi N, Yang XY, Mitra G, and Soman G. Characterization and analysis of thermal denaturation of antibodies by size exclusion high-performance liquid chromatography with quadruple detection. *Anal Biochem* **325**, 227-239, 2004.
[17] Hertadi R, Gruswitz F, Silver L, Koide A, Koide S, Arakawa H, and Ikai A. Unfolding mechanics of multiple OspA substructures investigated with single molecule force spectroscopy. *J Mol Biol* **333**, 993-1002, 2003.
[18] Murakoshi M, Iida K, Kumano S, and Wada H. Immune atomic force microscopy of prestin-transfected CHO cells using quantum dot. *Pflüger Archiv* (in press).
[19] Mio K, Kubo Y, Ogura T, Yamamoto T, Arisaka F, and Sato C. The motor protein prestin is a bullet-shaped molecule with inner cavities. *J Biol Chem* **283**, 1137-1145, 2008.
[20] Janovjak H, Kedrov A, Cisneros DA, Sapra KT, Struckmeier J, and Muller DJ. Imaging and detecting molecular interactions of single transmembrane proteins. *Neurobiol Aging* **27**, 546-561, 2006.
[21] Klug A, Rhodes D, Smith J, Finch JT, and Thomas JO. A low resolution structure for the histone core of the nucleosome. *Nature* **287**, 509-516, 1980.
[22] Csordas A. On the biological role of histone acetylation. *Biochem J* **265**, 23-38, 1990.
[23] Grunstein M. Histone acetylation in chromatin structure and transcription. *Nature* **389**, 349-352, 1997.
[24] Sterner DE and Berger SL. Acetylation of histones and transcription-related factors. *Microbiol Mol Biol Rev* **64**, 435-459, 2000.
[25] Villar-Garea A and Esteller M. Histone deacetylase inhibitors: understanding a new wave of anticancer agents. *Int J Cancer* **112**, 171-178, 2004.
[26] Ishihara K, Hong J, Zee O, and Ohuchi K. Mechanism of the eosinophilic differentiation of HL-60 clone 15 cells induced by n-butyrate. I*nt Arch Allergy Immunol* **137**(Suppl 1), 77-82, 2005.
[27] Riggs MG, Whittaker R, Neumann JR, and Ingram VM. *n*-Butyrate causes histone modification in HeLa and Friend erythroleukaemia cells. *Nature* **268**, 462-464, 1977.
[28] Yoshida M, Nomura S, and Beppu T. Effects of trichostatins on differentiation of murine erythroleukemia cells. *Cancer Res* **47**, 3688-3691, 1987.
[29] Darkin-Rattray SJ, Gurnett AM, Myers RW, Dulski PM, Crumley TM, Allocco JJ, Cannova C, Meinke PT, Colletti SL, Bednarek MA, Singh SB, Goetz MA, Dombrowski AW, Polishook JD, and Schmatz DM. Apicidin: a novel antiprotozoal agent that inhibits parasite histone deacetylase. *Proc Natl Acad Sci USA* **93**, 13143-13147, 1996.
[30] Izumi T, Kishimoto S, Takano T, Nakamura M, Miyabe Y, Nakata M, Sakanaka C, and Shimizu T. Expression of human platelet-activating factor receptor gene in EoL-1 cells following butyrate-induced differentiation. *Biochem J* **305**, 829-835, 1995.
[31] Hara K, Hasegawa T, Ooi H, Koya T, Tanabe Y, Tsukada H, Igarashi K, Suzuki E, Arakawa M, and Gejyo F. Inhibitory role of eosinophils on cell surface plasmin generation by bronchial epithelial cells: inhibitory effects of transforming growth factor β. *Lung* **179**, 9-20, 2001.
[32] Ishihara K, Hong J, Zee O, and Ohuchi K. Possible mechanism of action of the histone deacetylase inhibitors for the induction of differentiation of HL-60 clone 15 cells into eosinophils. *Br J Pharmacol* **142**, 1020-1030, 2004.
[33] Saito H, Bourinbaiar A, Ginsburg M, Minato K, Ceresi E, Yamada K, Machover D, Breard J, and Mathe G. Establishment and characterization of a new human eosinophilic leukemia cell line. *Blood* **66**, 1233-1240, 1985.
[34] KomatsuY, Tomizaki K, Tsukamoto M, Kato T, Nishino N, Sato S, Yamori T, Tsuruo T, Furumai R, Yoshida M, Horinouchi S, and Hayashi H. Cyclic hydroxamic-acid-containing peptide 31, a potent synthetic histone deacetylase inhibitor with antitumor activity. *Cancer Res* **61**, 4459-4466, 2001.
[35] Hong JJ, Ishihara K, Yamaki K, Hiraizumi K, Ohno T, Ahn JW, Zee OP, and Ohuchi K. Apicidin, a histone deacetylase inhibitor, induces differentiation of HL-60 cells. *Cancer Lett* **189**, 197-206, 2003.
[36] Cioe L, McNab A, Hubbell HR, Meo P, Curtis P, and Rovera G. Differential expression of the globin genes in human leukemia K562(S) cells induced to differentiate by hemin or butyric acid. *Cancer Res* **41**, 237-243, 1981.
[37] Witt O, Monkemeyer S, Ronndahl G, Erdlenbruch B, Reinhardt D, Kanbach K, and Pekrun A. Induction of fetal hemoglobin expression by the histone deacetylase inhibitor apicidin. *Blood* **101**, 2001-2007, 2003.